

5th International Conference on Computer Science and Computational Intelligence 2020

Long Short-Term Memory Algorithm for Rainfall Prediction Based on El-Nino and IOD Data

Dina Zatusiva Haq^a, Dian Candra Rini Novitasari^{b,*}, Abdulloh Hamid^c, Nurissaidah Ulinnuha^d, Arnita^e, Yuniar Farida^f, RR. Diah Nugraheni^g, Rinda Nariswari^h, Ilhamⁱ, Hetty Rohayani^j, Rahmat Pramulya^k, Ari Widjayanto^l

^{a,b,c,d,f} Department of Mathematics, UIN Sunan Ampel, Surabaya, Indonesia, 60237

^e Department of Mathematics, Universitas Negeri Medan, Medan, Indonesia, 20221

^g Department of Environmental Engineering, UIN Sunan Ampel, Surabaya, Indonesia, 60237

^h Statistics Department, School of Computer Science, Bina Nusantara University, Jakarta, Indonesia, 11480

ⁱ Department of Information System, UIN Sunan Ampel, Surabaya, Indonesia, 60237

^j Department of Information Technology, Adiwangsa Jambi University, Jambi, Indonesia, 36125

^k Faculty of Agriculture, University Teuku Umar, Aceh, Indonesia

^l Meteorological Climatological and Geophysics Agency, Surabaya, Indonesia, 60165

Abstract

Rainfall has the highest correlation with adverse natural disasters. One of them, rainfall can cause damage to the hot mud embankments in Sidoarjo, East Java, Indonesia. Therefore, in this study, rainfall prediction is carried out to anticipate the damage to the embankments. The rainfall prediction was carried out using Long Short-Term Memory (LSTM) based on rainfall parameters: El-Nino and Indian Ocean Dipole (IOD). Experiments were carried out with two schemes: the first scheme used the El-Nino and IOD parameters, while the second scheme used rainfall time series pattern. Each scheme used varied number of hidden layers, batch size, and learn drop period. The prediction results using El-Nino and IOD parameters obtained MAAPE values of 0.9644 with hidden layer, batch size and learn rate drop period values of 100, 64, and 50. The prediction results using rainfall parameters resulted in a more accurate prediction with a MAAPE value of 0.5810. The best prediction results were obtained with the number of hidden layers, batch size and learn rate drop period of 100, 32, and 150 respectively.

© 2021 The Authors. Published by Elsevier B.V.

This is an open access article under the CC BY-NC-ND license (<https://creativecommons.org/licenses/by-nc-nd/4.0>)

Peer-review under responsibility of the scientific committee of the 5th International Conference on Computer Science and Computational Intelligence 2020

Keywords: Deep Learning, Long Short-Term Memory, LSTM, Rainfall, Forecasting

* Corresponding author.

E-mail address: diancrini@uinsby.ac.id

1. Background

Rainfall in Indonesia has very high variability¹. This rainfall variability is influenced by El Nino and Indian Ocean Dipole (IOD) symptoms². El Nino symptom causes a reduction in the number of clouds formed resulting in a longer dry season in Indonesia. IOD is a phenomenon in which there is an interaction between the sea and the atmosphere around the equator in the Indian Ocean. This interaction results in a drastic decline in sea surface temperature around the south coast of Java and the west coast of Sumatra³. During the dry season, rainfall has a strong correlation with sea surface temperature. Meanwhile, during the rainy season, rainfall does not correlate with sea surface temperature².

Rainfall is highly influential in various sectors, such as agriculture, development, water resources, industry, and others⁴. Rainfall has the highest correlation with adverse natural disasters⁵. One of them is mud puddle disaster that has occurred since September 2006 in Sidoarjo, about 30 km south of Surabaya, East Java, Indonesia. The mud puddles can extend to surrounding areas. The expansion of the mud puddle area is prevented by the construction of hot mud embankments; however the embankments are only made of soil and unstable gravel. Gravel instability can cause damage to the embankments. Other factors that can cause damage to the embankments include soil displacement and high rainfall⁶. Therefore, prediction of rainfall is very important to do in order to anticipate damage to the embankments which can cause the expansion of the Lapindo mud puddle. Rainfall prediction has been conducted by previous researchers. Rainfall prediction by Binh Thai Pham in Hoa Binh Province is based on maximum temperature, minimum temperature, wind speed, relative humidity, and solar radiation as parameters by comparing several methods of artificial intelligence. The methods are Adaptive Neural Fuzzy Inference System optimized with Particle Swarm Optimization (PSOANFIS), Artificial Neural Network (ANN), and Support Vector Machine (SVM) with Mean Absolute Error (MAE) values in each method 3.281, 3.209, and 2.728⁷. The prediction methods that have been done by previous researchers are one of machine learning methods.

Deep learning is a part of machine learning that has several layers of computation allowing an algorithm to learn the representation of a data⁸. Deep learning significantly improves the quality of various computational applications such as pattern recognition, speech recognition, and object detection⁹. One of deep learning methods is Long Short-Term Memory (LSTM)¹⁰.

Long Short-Term Memory (LSTM) algorithm has been used by previous researchers. LSTM algorithm is used by Zheng et al. to estimate electricity load based on electricity consumption data and it has a better result than statistical methods such as SARIMA with Root Mean Square Error (RMSE) and Mean Absolute Percentage Error (MAPE) equals to 0.0702 and 0.0535¹¹. LSTM method is also used by Beibei Yang to predict landslide displacement by comparing the LSTM and SVM methods. The LSTM algorithm is better than SVM because LSTM algorithm can make connections in every state at different times, whereas the SVM algorithm only recognizes patterns at a one-time point, so the LSTM method is more suitable in time series data than SVM method¹². LSTM method by Xiangyun Qun to predict the duration of daily solar radiation using weather predictions shows better results on accuracy as much as 18.34% than the backpropagation method¹³. The research is carried out by Aswin S in predicting global average rainfall for 10368 geographical locations worldwide for 468 days by comparing two deep learning algorithms, LSTM and Convolutional Neural Network (ConvNet) based on the value of Mean Absolute Percentage Error (MAPE). The results indicate that the LSTM algorithm is better than the ConvNet algorithm, with MAPE values 1.6897 and 1.7281. The parameter used in this study was the average rainfall in one month at each different location¹⁰.

Based on the superiority of the LSTM algorithm in predicting time series patterns and the importance of rainfall prediction, the research on the prediction of rainfall in Sidoarjo, East Java using the LSTM algorithm is carried out. Mitigation of a disaster caused by high rainfall is required, considering that in Sidoarjo there is a mud embankment which is prone to landslides. This research is expected to be used as a reference for the community and government to anticipate the damage to the mud embankments due to the high rainfall in Sidoarjo, East Java.

2. Methodology

2.1 Research Parameter

Rainfall prediction requires data as parameters and target variable. This research uses two parameters, namely El Nino Index 3.4 and Indian Ocean Dipole (IOD) weekly data from 29 December 2014 to 4 August 2019 collected from

the Bureau of Meteorology (BOM). Target variable is daily rainfall data collected from Class I Meteorological Station Juanda Surabaya. Data samples are shown in Table 1.

Table 1 Sample data parameter dan variabel target

| <i>Index El-Nino 3.4</i> | <i>Indian Ocean Dipole (IOD)</i> | <i>Curah Hujan Harian</i> |
|--------------------------|----------------------------------|---------------------------|
| 0.5 | -0.46 | 0 |
| 0.37 | -0.34 | 8888 |
| 0.49 | -0.34 | |
| 0.5 | -0.34 | 62,3 |
| 0.39 | -0.73 | 91,9 |

Indian Ocean Dipole (IOD) and El-Nino are phenomena in the Indo Pacific Ocean that play an important role in the rainfall variability in Indonesia. IOD is a phenomenon in which there is an abnormal increase of sea surface temperature in the Indian Ocean south of India. This phenomenon is accompanied by an abnormal decline of sea surface temperature in Indonesian waters. El-Nino is a phenomenon in which there are changes of atmospheric pressure differences in the tropical regions of the Eastern Pacific Ocean (Mareta, Hidayat, Hidayati, & Alsepan, 2019). Rainfall is the amount of rain that falls in an area in a certain period. Rainfall is measured in millimeters from a flat surface which is not a catchment area and where evaporation or drainage does not occur¹⁵. According to the Meteorology, Climatology and Geophysics Agency (BMKG), rainfall in Indonesia is divided into 4 criteria as shown in Table 2

Table 2 Rainfall category

| Category | Notes |
|--------------------|--|
| Light rain | 1 - 5 mm / hour or 5 - 20 mm / day |
| Moderate rain | 5 - 10 mm / hour or 20 - 50 mm / day |
| Heavy rain | 10 - 20 mm / hour or 50 - 100 mm / day |
| Extreme heavy rain | > 20 mm / hour or > 100 mm / day |

2.2 Analytical Steps

The steps to predict rainfall using the LSTM algorithm are as follows:

2.2.1 Long Short-Term Memory (LSTM)

Recurrent Neural Network (RNN) is a part of Deep Learning containing a recurring connection in each unit of the hidden layer which is interconnected in every different time¹². RNN consists of hidden state h with optional output y and repeats as much as $x = (x_1, \dots, x_t)$. Hidden state $h_{(t)}$ in the RNN algorithm is updated every step t ¹⁶. The formula used to update the hidden state $h_{(t)}$ is shown in Eq. (3)¹⁷.

$$h_{(t)} = f(h_{t-1}, x_t) \quad (1)$$

Where f is non-linear activation function.

Long Short-Term Memory (LSTM) is a modification of the RNN method. The LSTM architecture aims to reduce the long-term dependency on the RNN algorithm by using memory cells to maintain the state for a long time¹⁷. The basic unit of Long Short-Term Memory is called a memory cell where each cell has a linear unit with a weight constant¹⁸. According to¹⁹ the steps of forming LSTM model are shown in Eq. (2) – Eq. (8).

$$f_t = \sigma(W_f \cdot [h_{t-1}, x_t] + b_f) \quad (2)$$

Where f_t is a forget gate, σ is sigmoid function, x_t is input value in t order, W_f is the weight of forget gate, b_f is bias value on forget gate, and h_t is output value in t order. The output of the t model is obtained from the output of the previous model or $t-1$ model $t-1$. Sigmoid function is defined by Eq. (3)

$$\sigma(x) = \frac{e^x - e^{-x}}{e^x + e^{-x}} \quad (3)$$

The model then determines which information will be stored. This process consists of two layers, the input gate layer and the sigmoid layer. Each layer serves to identify which values will be updated and form a vector containing the possibilities of new values. The merging of these two processes creates a new input value.

$$i_t = \sigma(W_i \cdot [h_{t-1}, x_t] + b_i) \quad (4)$$

$$\bar{C}_t = \tanh(W_c \cdot [h_{t-1}, x_t] + b_c) \quad (5)$$

$$C_t = C_t * C_{t-1} + i_t * \bar{C}_t \quad (6)$$

The output value is the selected value by the sigmoid gate.

$$o_t = \sigma(W_o \cdot [h_{t-1}, x_t] + b_o) \quad (7)$$

$$h_t = o_t * \tanh(C_t) \quad (8)$$

Where \tanh is used to scale values in the range -1 to 1, W_i is a weight of *input gate*, b_i bias value on input gate, \bar{C}_t is a new value that can be added to the cell state, C_t is the cell state, b_o bias value on cell state, and o_t is the output gate. The generated output of the model is the selected output based on the cell state model. The architecture of the LSTM algorithm is shown in Figure 1

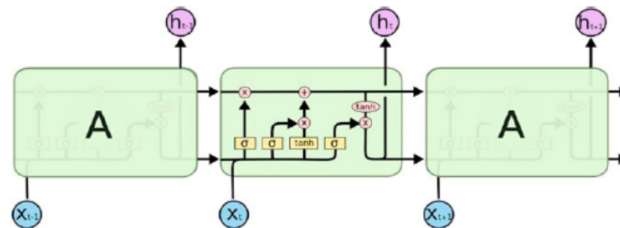


Figure 1 Architecture of LSTM [10]

2.2.2 Mean Arctan Absolute Percentage Error (MAAPE)

Mean Arctangent Absolute Percentage Error (MAAPE) is an equation to calculate the error value of predicted results. This function is more superior than the Mean Absolute Percentage Error (MAPE) to calculate error values. MAAPE allows target variable with zero values and a limited range of values so that the network training process is easier²⁰. MAAPE calculations are formulated by Eq. (9)

$$MAAPE = \frac{1}{N} \sum_{i=1}^N \arctan\left(\left|\frac{y_i - f_i}{y_i}\right|\right) \quad (9)$$

Where y_i is the original data, f_i is the predicted data, and N is the number of predicted data. The range of MAAPE value is 0 to $\pi/2$. Smaller MAAPE value indicates a more accurate prediction model²¹.

3. Result and Discussions

In this research, 240 weekly data from 29 December 2014 to 4 August 2019 were used. El Nino Index Data 3.4 and Indian Ocean Dipole were used as parameters to predict rainfall. The rainfall data collected from BMKG Juanda had some missing values. filling missing data can be carried out using interpolation method²². Daily rainfall data need to be accumulated into weekly data to obtain data in the same week as El-Nino Index 3.4 and IOD data. Each parameter is normalized by Z-score normalization²³. Normalization results for each parameter are shown in Table 3.

Table 3 Sample of normalized data

| Index El-Nino | Indian Ocean Dipole (IOD) | Rainfall |
|---------------|---------------------------|----------|
| -0.0078 | -0.9754 | 0.4612 |
| -0.1656 | -0.7017 | 0.3731 |
| -0.0200 | -0.7017 | 0.4480 |
| -0.0078 | -0.7017 | 2.0269 |
| -0.1413 | -1.5912 | 1.6307 |

LSTM networks are trained by input data and target variable. In this research, two trials were conducted to make the patterns of the input data and target variable. The first trial of input data was sequential vector Indexes of the El-Nino (E) and IOD (I), while the target variable was taken from rainfall data (C). The input data and the target variable of the first trial were treated as shown in Table 4.

The second trial predicts rainfall at one time based on sequential data of the previous rainfall. The target data from the second trial is rainfall in the sequence after the input data. The second trial only used time-series data of rainfall. The input and target variable in the trial with rainfall parameter were treated as shown in Table 4.

Table 4 Input data pattern with El-Nino and IOD parameters

| <i>Dataset E</i> | <i>Dataset I</i> | <i>Sequential Vector</i> | <i>Target</i> |
|---|---|--|---------------|
| E_1, E_2, E_3, E_4, E_5 | I_1, I_2, I_3, I_4, I_5 | $E_1, E_2, E_3, E_4, E_5, I_1, I_2, I_3, I_4, I_5$ | C_6 |
| E_2, E_3, E_4, E_5, E_6 | I_2, I_3, I_4, I_5, I_6 | $E_2, E_3, E_4, E_5, E_6, I_2, I_3, I_4, I_5, I_6$ | C_7 |
| \vdots | \vdots | \vdots | \vdots |
| $E_{235}, E_{236}, E_{237}, E_{238}, E_{239}$ | $I_{235}, I_{236}, I_{237}, I_{238}, I_{239}$ | $E_{235}, E_{236}, E_{237}, E_{238}, E_{239}, I_{235}, I_{236}, I_{237}, I_{238}, I_{239}$ | C_{240} |

Table 5 Input data pattern with rainfall parameter

| <i>Dataset C</i> | <i>Target</i> |
|---|---------------|
| C_1, C_2, C_3, C_4, C_5 | C_6 |
| C_2, C_3, C_4, C_5, C_6 | C_7 |
| \vdots | \vdots |
| $C_{235}, C_{236}, C_{237}, C_{238}, C_{239}$ | C_{240} |

LSTM has several parameters affecting prediction results such as a hidden layer, batch size and learn rate drop period. The hidden layer is the number of calculations in the training process conducted, batch size is used to set how often the weight on the network will be updated, and the learn rate drop period is the number of repetitions to determine learning rate. The architecture of LSTM algorithm in this research is shown in Figure 2, where that E is El-Nino data, I is IOD data, x_t is treated input data, i_t is the input gate, C_t is the cell state, o_t is the output gate, M is the number of hidden layers, and y_t is the target variable.

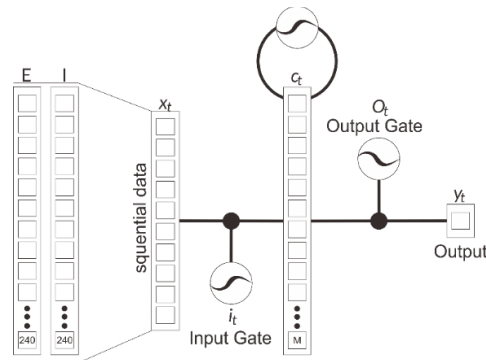


Figure 2 Architecture of LSTM for rainfall prediction

The division of data also influences the prediction results. The data division in the trial conducted with input data pattern using El-Nino and IOD parameters and rainfall parameter shows that the 60% training data achieved the smallest MAAPE value in each input data pattern. The 60% training data was also experimented with hidden layer variations, batch size, and learn rate drop periods to obtain the best prediction results. The MAAPE values for each experiment are shown in Table 6 and Table 7.

Based on Table 6, it can be seen that the average MAAPE value on each hidden layer is not much different. The lowest average MAAPE value is 0.9681, with 300 hidden layers. The lowest MAAPE value with 300 hidden layers is 0.9720, with 256 batch size value, and 50 learn rate drop period, while the highest MAAPE value with 300 hidden layers, 32 batch size, and 50 learn rate drop period is 0.9990. The highest average MAAPE value with 200 hidden layers is 0.9923. The lowest MAAPE value with 200 hidden layers, 256 batch size value and 50 learn rate drop period is 0.9677, while the highest MAAPE value with 200 hidden layers, 32 batch size value and 50 learn rate drop period is 1.0259. For 100 hidden layers, the lowest MAAPE value is 0.9644 with 64 batch size and 50 learn rate drop period, while the highest MAAPE value is 1.0288 with 128 batch size and 150 learn rate drop periods. Overall, the lowest MAAPE value is 0.9644. The results of rainfall prediction with the lowest MAAPE value are visualized in Figure 3 (a).

Based on Table 7, it can be seen that the more the hidden layers, the lower the MAAPE value, and the lower the batch size value, the lower the MAAPE value. On the other hand, the higher learn rate drop period value, the lower

the MAAPE value. Each hidden layer has an average MAAPE value which is not much different. The lowest average MAAPE value is 0.6218, with 300 hidden layers. The lowest MAAPE value with 300 hidden layers, 32 batch size, and 150 learn rate drop period is 0.5810, while the highest MAAPE value with 300 hidden layers, 256 batch size, and 50 learn rate drop period is 0.6529. The highest average of MAAPE value is 0.6218, with 100 hidden layers. The smallest MAAPE value with 100 hidden layers, 32 batch size, and 150 learn rate drop period is 0.5940, while the highest MAAPE value with 100 hidden layers, 256 batch size, and 50 learn rate drop period is 0.6884. The average MAAPE value with 200 hidden layers is 0.6253. The lowest MAAPE value with 200 hidden layers, 32 batch size, and 150 learn rate drop period is 0.5850, while the highest MAAPE value with 100 hidden layers, 256 batch size, and 50 learn rate drop period is 0.6541. Overall the smallest MAAPE value is 0.5810. The results of rainfall prediction with the lowest MAAPE value are visualized in Figure 3 (b).

Table 6 MAAPE value using El-Nino and IOD parameters

| Hidden Layers | Batch Size | Learn Rate Drop Period | MAAPE | Average |
|---------------|------------|------------------------|--------|---------|
| 100 | 256 | 50 | 0.9680 | 0.9889 |
| | | 100 | 0.9847 | |
| | | 150 | 0.9851 | |
| | 128 | 50 | 0.9707 | |
| | | 100 | 0.9977 | |
| | | 150 | 1.0288 | |
| | 64 | 50 | 0.9644 | |
| | | 100 | 0.9825 | |
| | | 150 | 0.9974 | |
| | 32 | 50 | 0.9715 | |
| | | 100 | 1.0047 | |
| | | 150 | 1.0116 | |
| 200 | 256 | 50 | 0.9677 | 0.9923 |
| | | 100 | 0.9862 | |
| | | 150 | 0.9982 | |
| | 128 | 50 | 0.9829 | |
| | | 100 | 0.9871 | |
| | | 150 | 0.9926 | |
| | 64 | 50 | 0.9796 | |
| | | 100 | 0.9970 | |
| | | 150 | 1.0012 | |
| | 32 | 50 | 0.9903 | |
| | | 100 | 0.9999 | |
| | | 150 | 1.0259 | |
| 300 | 256 | 50 | 0.9720 | 0.9681 |
| | | 100 | 0.9928 | |
| | | 150 | 0.9744 | |
| | 128 | 50 | 0.9760 | |
| | | 100 | 0.9877 | |
| | | 150 | 0.9958 | |
| | 64 | 50 | 0.9920 | |
| | | 100 | 0.9958 | |
| | | 150 | 0.9739 | |
| | 32 | 50 | 0.9990 | |
| | | 100 | 0.9961 | |
| | | 150 | 0.9782 | |

The graph in Figure 3 (a) shows the results of testing data prediction from October 16, 2017 to August 4, 2019. The results of prediction using the pattern of input data with El-Nino and IOD parameters are the predicted data has a similar pattern to the actual data, but the difference between the actual data and the predicted data is quite significant. Prediction results indicate the occurrence of high rainfall on October 16, 2017 to October 8, 2018 with an average rainfall of 58.4798 mm. Rainfall increased again from February 10, 2019 to May 12, 2019 with an average rainfall of 82.0113 mm. The increase of the rainfall prediction is similar to the increase of the rainfall in the actual data. The rainfall of the real data increased from October 16, 2017 to July 16, 2018 with an average rainfall of 69.4271 mm. The rainfall rose again on November 20, 2018 to April 28, 2019 with an average rainfall of 102,2023 mm.

The graph in Figure 3 (b) shows the prediction results using rainfall parameters. It has a very similar pattern to the actual data, so the predicted results are assumed to be good and are the best result of all experiments conducted with the calculation of the MAAPE value of 0.5810. Prediction results indicate the occurrence of high rainfall from October 16, 2017, to July 16, 2018, with an average rainfall of 69.5658 mm. The rainfall increased again from November 20, 2018, to April 28, 2019, with an average rainfall of 102.1778 mm. The increase in rainfall of the prediction results is similar to the rainfall of the actual data. The rainfall of the actual data increased from October 16, 2017 to July 16, 2018, with an average rainfall of 69.4271 mm. The rainfall increased again from November 20, 2018, to April 28, 2019, with an average rainfall of 102,2023 mm. Based on the two graphs in Figure 3, it is shown that the best prediction results are performed using a data input pattern with rainfall parameters where the LSTM algorithm is trained only using rainfall parameter. The MAAPE value of 0.9644 on the prediction results using the El-Nino and IOD parameters shows that El-Nino and IOD are not strong enough to predict rainfall in Sidoarjo area, East Java. El-Nino and IOD have a strong influence on rainfall patterns in areas close to the Indian Ocean. The area covered by the El-Nino and IOD phenomena in Indonesia is an area that has an equatorial rain type. Areas that are equatorial rain types, like Sumatra, Kalimantan, Papua and Sulawesi, which is crossed by the equator, whereas Sidoarjo has monsoon rain type. In addition, El-Nino phenomenon does not occur every year, but this phenomenon will appear every three or seven years. The El-Nino phenomenon is also influenced by the east and west monsoon winds³. Rainfall can be predicted based on other factors such as temperature, relative humidity, and wind speed¹⁵ and also can be predicted using image data based on the Himawari-8 IR satellite²⁴.

Table 7 MAAPE values using rainfall parameter

| Hidden Layers | Batch Size | Learn Rate Drop Period | MAAPE | Average |
|---------------|------------|------------------------|--------|---------|
| 100 | 256 | 50 | 0.6884 | 0.6299 |
| | | 100 | 0.6416 | |
| | | 150 | 0.6256 | |
| | 128 | 50 | 0.6631 | |
| | | 100 | 0.6489 | |
| | | 150 | 0.6177 | |
| | 64 | 50 | 0.6490 | |
| | | 100 | 0.6032 | |
| | | 150 | 0.6013 | |
| | 32 | 50 | 0.6327 | |
| | | 100 | 0.5940 | |
| | | 150 | 0.5940 | |
| 200 | 256 | 50 | 0.6541 | 0.6253 |
| | | 100 | 0.6427 | |
| | | 150 | 0.6225 | |
| | 128 | 50 | 0.6566 | |
| | | 100 | 0.6530 | |
| | | 150 | 0.6195 | |
| | 64 | 50 | 0.6377 | |
| | | 100 | 0.6155 | |
| | | 150 | 0.6007 | |
| | 32 | 50 | 0.6295 | |
| | | 100 | 0.5876 | |
| | | 150 | 0.5850 | |
| 300 | 256 | 50 | 0.6529 | 0.6218 |
| | | 100 | 0.6389 | |
| | | 150 | 0.6250 | |
| | 128 | 50 | 0.6522 | |
| | | 100 | 0.6403 | |
| | | 150 | 0.6153 | |
| | 64 | 50 | 0.6444 | |
| | | 100 | 0.6048 | |
| | | 150 | 0.5908 | |
| | 32 | 50 | 0.6220 | |
| | | 100 | 0.5950 | |
| | | 150 | 0.5810 | |

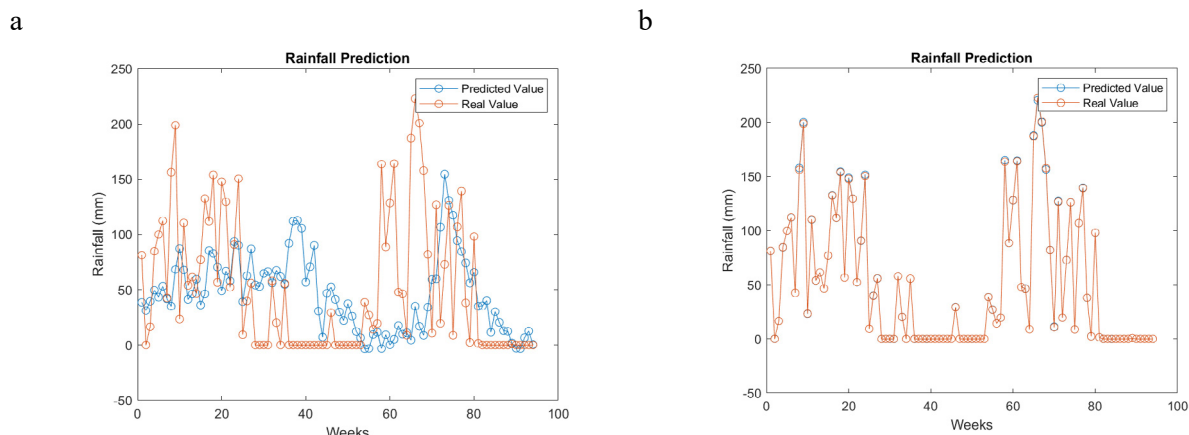


Figure 3 (a) Prediction result using El-Nino and IOD parameters, (b) Prediction result using rainfall parameter

4. Conclusions

The LSTM algorithm was applied to predict the rainfall in Sidoarjo, East Java. The Rainfall prediction used El-Nino and IOD parameters using five weekly El-Nino and IOD data to predict the rainfall data for the 6th week. The prediction using rainfall parameters was obtained from 5 weeks to predict the rainfall data for the 6th week. By using several LSTM algorithm parameters in the experiments such as hidden layer, batch size, and learn rate drop period, it is shown that the results of the prediction using the rainfall parameter was more accurate than using El-Nino and IOD parameters. The lowest MAAPE value obtained from the experiment conducted on the second data input pattern was 0.5810. The lowest MAAPE value when using El-Nino and IOD parameters was 0.9644. The prediction results with the MAAPE value of 0.9644 using the El-Nino and IOD parameters showed that El-Nino and IOD were strong enough to predict the rainfall in Sidoarjo area, East Java.

References

1. Wahid H. Analysis of the Characteristics and Classification of Rainfall in Polewali Mandar Regency. *Jurnal Sainsmat*. 2017; VI(1).
2. Lestari DO, Sutriyono E, Sabaruddin S, Iskandar I. Respective Influences of Indian Ocean Dipole and El Niño-Southern Oscillation on Indonesian Precipitation. *Journal of Mathematical and Fundamental Sciences*. 2018; 50(3).
3. Nur'utami MN, Hidayat R. Influences of IOD and ENSO to Indonesian rainfall variability: role of atmosphere-ocean interaction in the Indo-Pacific sector. *Procedia Environmental Sciences*. 2016; 33.
4. Rustiana S, Ruchjana BN, Abdullah AS, Hermawan E, Sipayung SB, Jaya IGNM, et al. Rainfall prediction of Cimanuk watershed regions with canonical correlation analysis (CCA). *Journal of Physics: Conference Series*. 2017; 893(1).
5. Echevarría Y, Sánchez L, Blanco C. Rainfall Prediction: A Deep Learning Approach. *Lecture Notes in Computer Science (including subseries Lecture Notes in Artificial Intelligence and Lecture Notes in Bioinformatics)*. 2016; 9648.
6. Istadi BP, Pramono GH, Sumintadireja P, Alam S. Modeling study of growth and potential geohazard for LUSI mud volcano: East Java, Indonesia. *Marine and Petroleum Geology*. 2009; 26(9).
7. Pham BT, Le LM, Le TT, Bui KTT, Le VM, Ly HB, et al. Development of advanced artificial intelligence models for daily rainfall prediction. *Atmospheric Research*. 2020; 237.
8. Poplin R, Varadarajan AV, Blumer K, Liu Y, McConnell MV, Corrado GS, et al. Prediction of cardiovascular risk factors from retinal fundus photographs via deep learning. *Nature Biomedical Engineering*. 2018; 2(3).
9. Lecun Y, Bengio Y, Hinton G. Deep Learning. *Nature*. 2015; 521(7533).
10. Aswin S, Geetha P, Vinayakumar R. Deep Learning Models for the Prediction of Rainfall. *Proceedings of the 2018 IEEE International Conference on Communication and Signal Processing, ICCSP 2018*. 2018.
11. Zheng J, Xu C, Zhang Z, Li X. Electric load forecasting in smart grids using Long-Short-Term-Memory based Recurrent Neural Network. *2017 51st Annual Conference on Information Sciences and Systems, CISS 2017*. 2017.
12. Yang B, Yin K, Lacasse S, Liu Z. Time series analysis and long short-term memory neural network to predict landslide displacement. *Landslides*. 2019; 16(4).
13. Qing X, Niu Y. Hourly day-ahead solar irradiance prediction using weather forecasts by LSTM. *Energy*. 2018; 148.

14. Mareta L, Hidayat R, Hidayati R, Alsepan G. Influence of the positive Indian Ocean Dipole in 2012 and El Niño-southern oscillation (ENSO) in 2015 on the Indonesian Rainfall Variability. *IOP Conference Series: Earth and Environmental Science*. 2019; 284(1).
15. Novitasari DCR, Rohayani H, Suwanto , Arnita , Rico , Junaidi R, et al. Weather Parameters Forecasting as Variables for Rainfall Prediction using Adaptive Neuro Fuzzy Inference System (ANFIS) and Support Vector Regression (SVR). *Journal of Physics: Conference Series*. 2020; 1501(1).
16. Asyhar AH, Foeady AZ, Thohir M, Arifin AZ, Haq DZ, Novitasari DCR. Implementation LSTM Algorithm for Cervical Cancer using Colposcopy Data. In ; 2020.
17. Sak H, Senior A, Beaufays F. Long short-term memory recurrent neural network architectures for large scale acoustic modeling. In ; 2014.
18. Kırbaş İ, Sözen A, Tuncer AD, Kazancıoğlu FŞ. Comparative analysis and forecasting of COVID-19 cases in various European countries with ARIMA, NARNN and LSTM approaches. *Chaos, Solitons and Fractals*. 2020; 138.
19. Moghar A, Hamiche M. Stock Market Prediction Using LSTM Recurrent Neural Network. *Procedia Computer Science*. 2020 170.
20. Hinch AZ, Tkouat M. A deep long-short-term-memory neural network for lithium-ion battery prognostics. In ; 2018.
21. Chen C, Liu H. Medium-term wind power forecasting based on multi-resolution multi-learner ensemble and adaptive model selection. *Energy Conversion and Management*. 2020; 206(1).
22. Moon T, Hong S, Choi HY, Jung DH, Chang SH, Son JE. Interpolation of greenhouse environment data using multilayer perceptron. 2019. ; 166(9).
23. Pollesch NL, Dale VH. Normalization in sustainability assessment: Methods and implications. *Ecological Economics*. 2016; 130.